

Electronic Supplementary Information

Tailoring of structural and photoluminescence emissions by Mn and Cu co-doping in 2D nanostructures of ZnS for visualization of latent fingerprints and generation of white light

Partha Kumbhakar^a, Subrata Biswas^a, Prafull Pandey^b, Chandra S. Tiwary^{c,d}, and Pathik Kumbhakar^{*a}

^aNanoscience Laboratory, Department of Physics, National Institute of Technology Durgapur, 713209, India

^bMaterials Engineering, Indian Institute of Science, Bangalore-560012, India.

^cDepartment of Materials Science and Engineering, Indian Institute of Technology Gandhinagar, Palaj 382355, Gujarat, India.

^dPresent Address: Metallurgical and Materials Engineering, Indian Institute of Technology Kharagpur, Kharagpur-721302, India

**Corresponding author: E-mail: pathik.kumbhakar@phy.nitdgp.ac.in & nitdgpkumbhakar@yahoo.com*

Contents

- S1. Analysis of XRD result and Strain calculation by using Williamson-Hall method**
- S2. Schematic illustration of sheet formation and size distributions of the synthesized samples**
- S3. HRTEM image analysis**
- S4. XPS analysis of the Mn-Cu co-doped ZnS samples**
- S5. Optical property analysis**
- S6. Photoluminescence quantum yield (PLQY) measurement**
- S7. Investigation on temperature dependent PL emissive behaviour of synthesized sample**
- S8. Analysis of PL decay curve**
- S9. The intensity profile of the aged luminescent fingerprints**
- S10. The luminescence profile of the fabricated WLED and its phototropic parameters calculation**

Analyses of XRD results and strain calculation by using Williamson-Hall method

To investigate the tensile strain (ϵ) developed in our samples we have calculated the strain by using the Williamson-Hall equation given below,¹

$$\epsilon = \frac{\beta_{hkl}}{4 \tan \theta} \quad (1)$$

Where, β_{hkl} is the full-width at half maximum (FWHM) of line broadening, θ is the peak position

By considering both of these broadenings, the calculated values are given below,

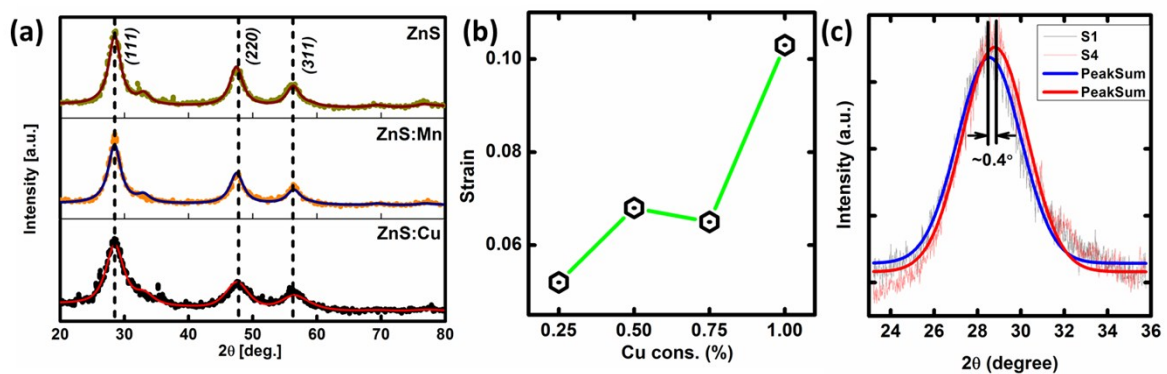


Fig. S1 (a) XRD pattern of ZnS, ZnS:Mn and ZnS:Cu NMs. (b) Strain plot with increase copper dopant concentration in ZnS:Mn. (c) XRD pattern shows the peak shift of (111) plane by using Gaussian fitting of S1 and S4 sample.

Table S1 The value of strain of all synthesized samples

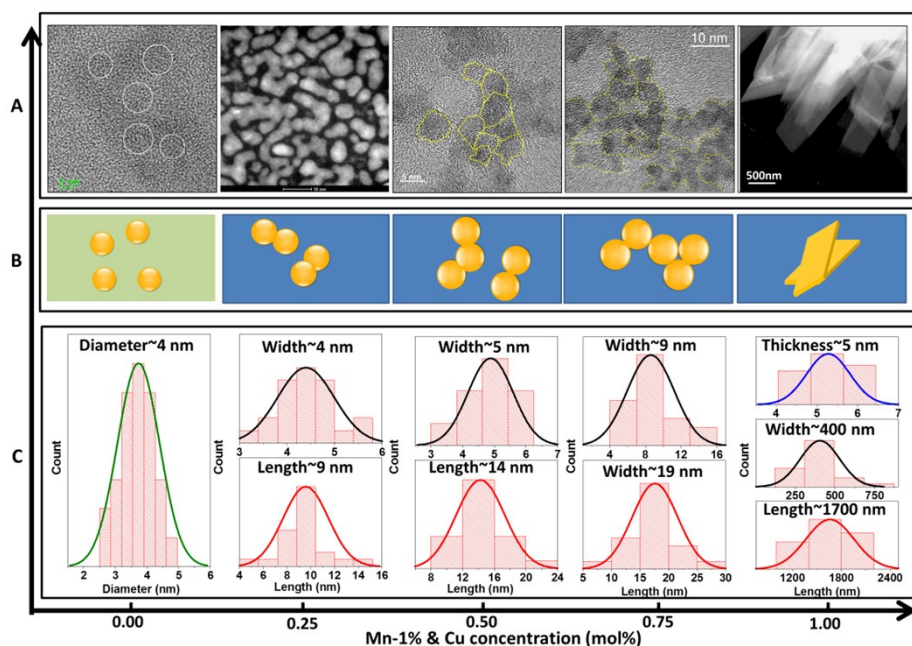
Sample	ZnS:Mn	S1	S2	S3	S4
a (Å)	5.37	5.31	5.39	5.33	5.36
β_{hkl}	0.0494	0.0529	0.0705	0.0667	0.1059
Strain (ϵ)	0.0481	0.0518	0.0679	0.0651	0.1025

The crystalline size has been calculated by using Debye-Scherrer equation¹ and the estimated values are found out to be 2.7 nm, 2.2 nm, 2.3 nm and 1.5 nm for S1, S2, S3 and S4, respectively.

$$D = \frac{k\lambda}{\beta_{hkl} \cos \theta} \quad (2)$$

Where, D is the crystalline size, k is shape factor and λ is the wavelength of radiation.

Schematic illustration of sheet formation and size distributions of the synthesized samples



Scheme S1: Overview of the obtained nanostructures. Panel A: from left to right: showing the TEM and HAADF images when different concentration of Cu precursor used. Panel B: showing the schematic illustration of the OA with the effect of dopant concentration. Panel C: size distribution of ZnS:Mn sample (left). Length and width have been calculated by log distribution of particles with varying the Cu concentration

HRTEM image analyses

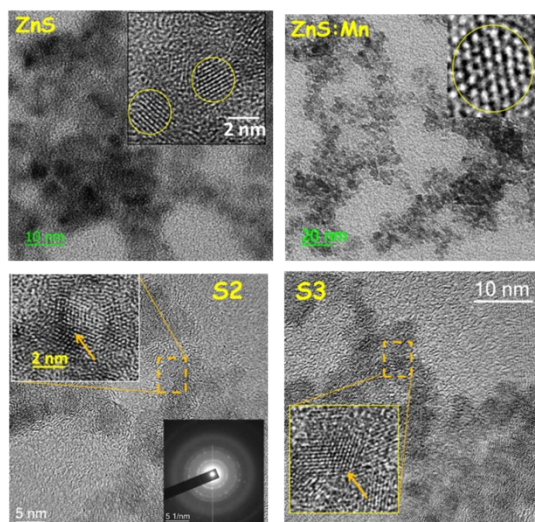


Fig. S2 HRTEM image of ZnS (a), Mn doped ZnS (b), S2 (c) and S3 sample (d). Inset shows the magnified image of all samples and SEAD pattern with lattice presence of defects.

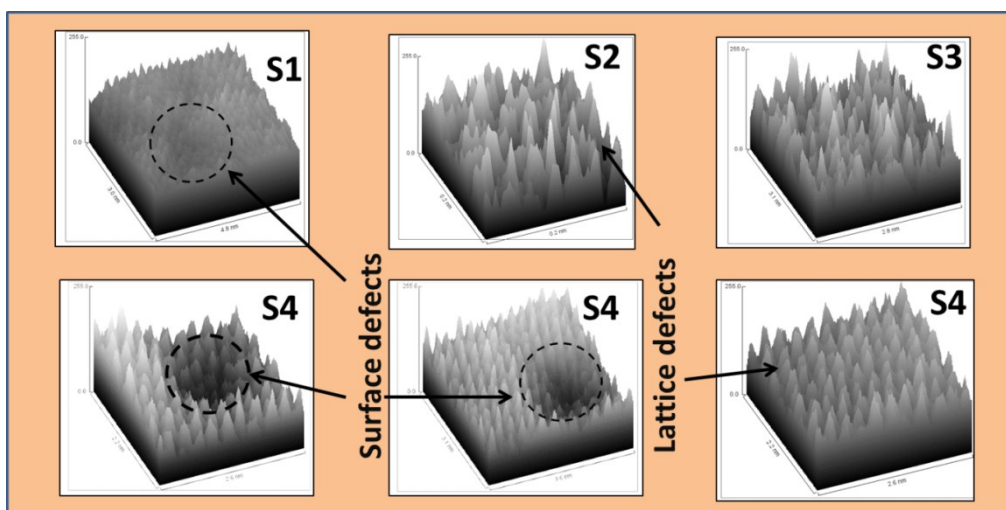


Fig.S3 Surface plot of all synthesized co-doped samples.

XPS analysis of the Mn-Cu co-doped ZnS samples

The percentage profile of the elements (Zn, S, Mn and Cu) present within the synthesized co-doped samples has been calculated and the corresponding bar-diagram has been shown in Fig. S4b. It is observed that from S1 to S4, the percentage of Cu is increased whereas the other elements remain almost constant.

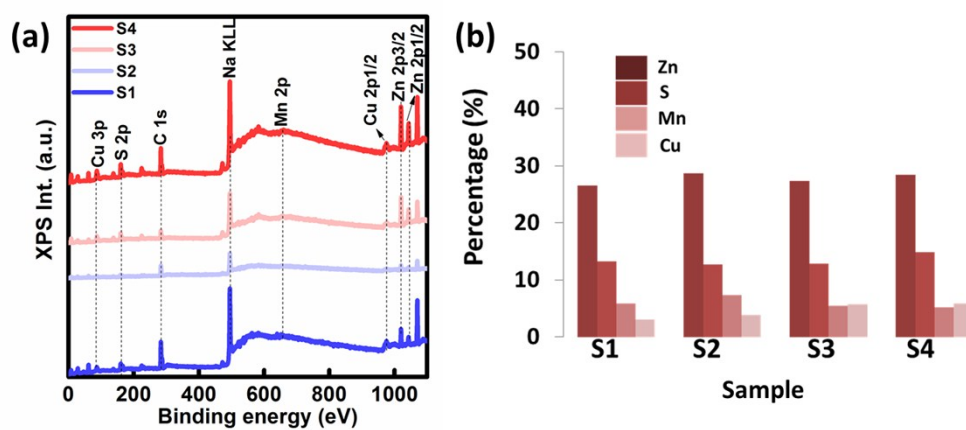


Fig. S4. XPS plot (a) and corresponding atomic percentage values (b) of the elements (Zn, S, Mn and Cu) of all synthesized co-doped samples.

Optical property

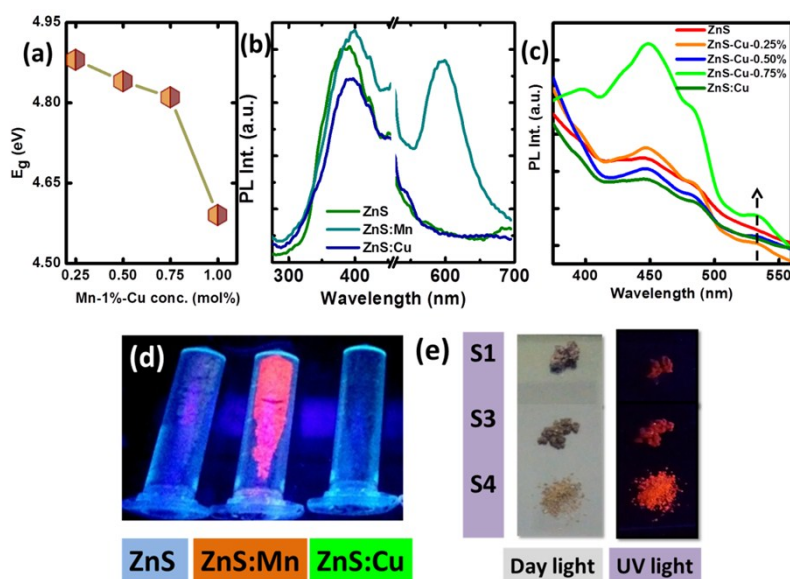


Fig. S5. (a) Energy band gap value of all synthesized sample with varying concentration Cu 0.25 to 1%.for co-doped sample.(b) PL emission spectra of un-doped ZnS, Mn doped ZnS and Cu doped ZnS sample.(c) PL emission spectra of all Cu-doped ZnS sample with varying concentration from 0 to 1%. (d) Digital photograph of the un-doped ZnS, Mn doped ZnS and Cu doped ZnS sample under UV light excitation. (e) Digital photograph of the co-doped ZnS samples under UV light and visible light excitation.

Photoluminescence quantum yield (PLQY) measurement

The PL quantum yields (PLQY) (Φ_s) of the synthesized doped sample has been calculated by comparing its integrated PL intensity (excited at 365 nm) and the absorbance value (at 365 nm) with that of the Rhodamine 6G (Rh6G) dispersed in water (0.1 μ M) of PLQY 95% employed as standard.² To determine the PLQY, 200 μ L of a ZnS:Mn-Cu aqueous solution (pH~6.7) was prepared by ultrasonication for 30 min to achieve a good dispersion and placed in a spectrofluorimeter (Perkin Elmer LS-55). The PLQY measurement has been performed under ambient atmosphere. For each sample, the emission is measured from 500 to 700 nm. The following equation been used to calculate the value of Φ_s of synthesized samples.

$$\phi_S = \phi_R \left[\frac{A_R(\lambda)I_S(\lambda)}{A_S(\lambda)I_R(\lambda)} \right] \frac{n_S^2}{n_R^2}. \quad (3)$$

Where Φ_S and Φ_R are the quantum yields of the sample and reference respectively; $A_R(\lambda)$ and $A_S(\lambda)$ are absorbance of the reference and sample respectively. $I_S(\lambda)$ and $I_R(\lambda)$ are the integrated PL intensities of sample and reference, respectively. Here n_S and n_R are the refractive index of the sample and reference medium respectively.

Table S2: PLQY of all co-doped samples at pH~6.7 and temperature 27°C.

	ZnS:Mn	S1	S2	S3	S4
Excitation (λ_{ex})	365 nm	365 nm	365 nm	365 nm	365 nm
PLQY (%)	42%	49%	62%	29%	29%

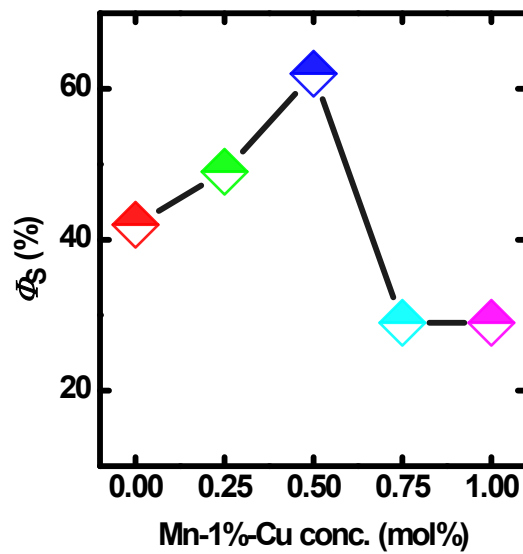


Fig. S6 PLQY of all synthesized sample with varying concentration of Cu 0 to 1%

Investigation on temperature dependent PL emissive behaviour of synthesized sample

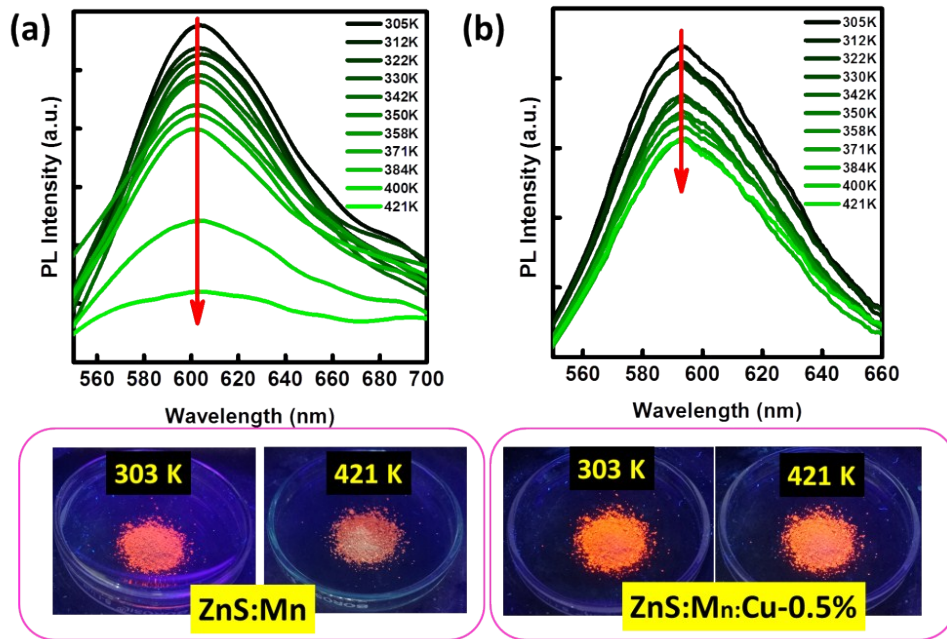


Fig. S7. (a) Temperature-dependent (305-421 K) PL spectra of ZnS:Mn and (b) ZnS:Mn:Cu-0.5% sample upon excitation at 365 nm. Lower panel shows the digital photographs of ZnS:Mn and ZnS:Mn:Cu-0.5% samples were recorded using a smart phone camera. All the measurements were carried out under the identical conditions

Analysis of PL decay curve

The average life time (τ_{av}) has been calculated by using these equations,³

$$\tau_{av} = \int_0^{\infty} I(t) dt \quad (4)$$

Where $I(t)$ is the normalized initial intensity of PL at time t .

The energy transfer efficiency can be calculated by,

$$\delta_{ET} = 1 - \frac{\tau_{DA}}{\tau_D} \quad (5)$$

and,

$$\frac{1}{\tau_{DA}} = \frac{1}{\tau_D} + k_{ET} \quad (6)$$

Where, t_{DA} , t_D , are PL lifetime for Mn with Cu and Mn without Cu in ZnS host. k_{ET} is energy transfer rate.

Table S3 Decay time of all co-doped samples and energy transfer rates

Species	τ_{Mn} (μs)	τ_{Cu} (μs)	δ_{ET}
ZnS:Mn	82		
S1	12	8	86%
S2	37	7	54%
S3	9	5	89%
S4	12	7	86%

The intensity profile of the aged luminescent fingerprints treated with ZnS:Mn-Cu and RhB dye

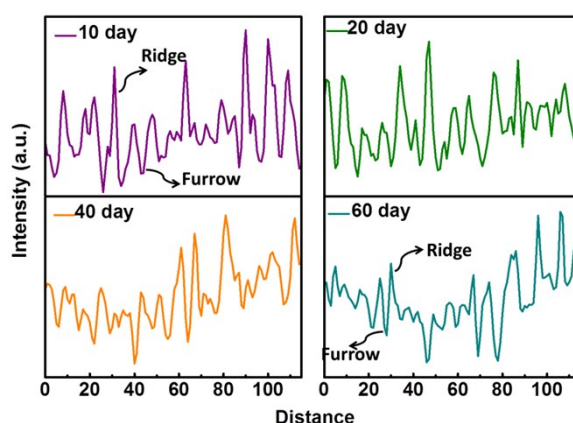


Fig. S8. The intensity variation of all aged fingerprints developed using S2 sample.

Fluorescent dyes are basically used to detect the LFPs⁴, so here a comparison of performance of synthesized ZnS:Mn-Cu sample and a highly fluorescent dye namely, Rhodamine B (RhB) for detection of aged LFPs have been made and results are shown in Fig. S9. It can be seen from Fig. S9 that, initially (denoted by 0 dye), the ridge patterns of the two LFPs stained by ZnS:Mn-Cu sample (left) and RhB dye (right) are almost similar. But in case of 20 day aged LFPs developed by synthesized sample, the intensity profile is much clearer and ridge-furrow patterns are easily visualized in compared to those of dye stained LFPs. The dimmed fluorescence intensity of ridge-furrow pattern, developed by RhB dye, may have aroused due to the intensity loss, aggregation of dye particles, temperature, low selectivity, atmospheric contamination, light exposure, hydrophilic nature,

radiation and dust during storage in the laboratory environment, etc.⁵⁻⁶. The clear variation of intensity value over the ridge-furrow pattern of fingerprints even after 20 days aging suggests that the S2 sample displays high contrast ratio due to the high selectivity and strong interaction between the synthesized sample and fingerprint residue.

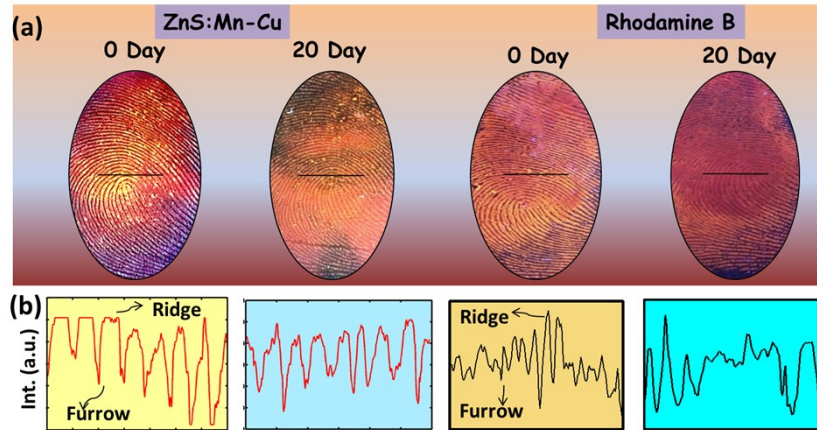


Fig. S9: (a) Upper panel shows the digital images of LFPs at freshly deposited fingerprints and 20 days old fingerprints treated with the ZnS:Mn-Cu (left) and RhB dye (right), respectively. (b) Lower panel shows the variation of intensity value over the fingerprints as indicated by the solid black lines.

The luminescence profile of the fabricated WLED and its property analysis

The desirable optical properties of the S3 (Mn-1% & Cu-0.75%) sample encourage us to fabricate WLED by combined with an n-UV LED chip ($\lambda=390\text{nm}$). However, a single type of colour converting material has tremendous advantages over multiple component ones, such as simple fabrication methods, low-cost fabrication techniques, variation of chromaticity coordinates by easily changing the materials and so on.⁷⁻⁹ Here, we have fabricated four different WLED by using appropriate concentration of the sample and PVA hydrogel coated on the LED chip (details in the Experimental section). The XYZ colour space values have been calculated by tristimulus values (X, Y and Z) and the tristimulus values can be calculated from the emission spectrum using the CIE colour-matching functions. The chromaticity coordinates x and y were obtained as follows,⁸

$$x = \frac{X}{X + Y + Z} . \quad (7)$$

$$y = \frac{Y}{X+Y+Z}. \quad (8)$$

The Luminous efficacy of radiation or luminous flux is the efficiency of energy conversion from electrical power to optical power. The luminous efficacy of radiation (lmW^{-1}) has been calculated through the following equation,⁹

$$LE(\text{lmW}^{-1}) = 683 \text{LW}^{-1} \times \frac{\int V(\lambda)S(\lambda)d\lambda}{\int S(\lambda)d\lambda}. \quad (9)$$

$V(\lambda)$ is the spectral luminous efficiency of photopic vision and $S(\lambda)$ is the spectral power distribution (SPD), which describes the power per unit area per unit wavelength of WLEDs. Due to strong interactions between the synthesized sample and polymer, highly stable PL properties have been obtained. The luminescence spectra of other co-doped sample also have shown in Fig. S10a-c.

Table S4 Phototropic parameter such as CIE, CCT, LE of all fabricated WLED

Sample	CIE colour coordinates	CCT (K)	LE (lm W^{-1})
S1	(0.25,0.27)	1848	40.98
S2	(0.28,0.43)	4227	62.14
S3	(0.31,0.32)	5406	94.95
S4	(0.25,0.36)	3039	76.90

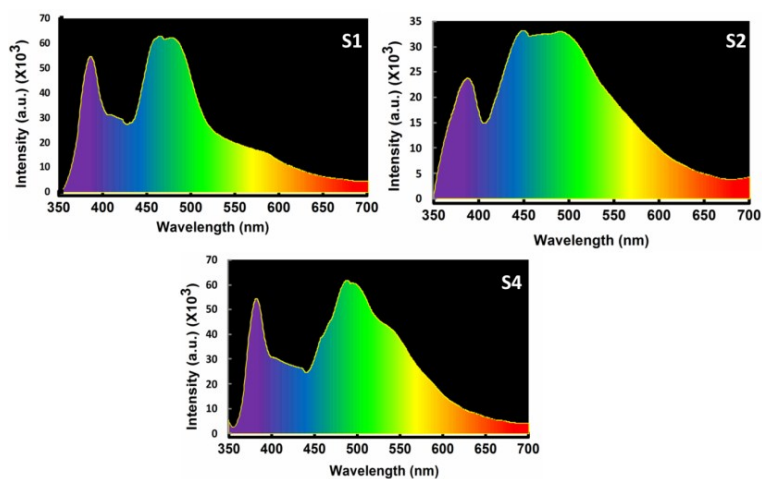


Fig. S10 (a-c) Emission spectra n-UV LED chip after coating with S1, S2 and S4 sample with an input voltage of 3.8 V.

References:

1. D. Verma, A. K. Kole, P. Kumbhakar, *J. Alloys Compd.*, 2015, **625**, 122-130.
2. R. F. Kubin, A. N. Fletcher, *J. Lumin.*, 1982, **27**, 455-462.
3. J. R. Lakowicz, *Principles of fluorescence spectroscopy*. 3rd ed. Springer-Verlag: Berlin. 2006.
4. G. S. Sodhi, J. Kaur, R. K. Garg, *J Forensic Ident.*, 2003, **53**, 551-555.
5. A. Becue, *Anal. Methods.*, 2016, **8**, 7983-8003.
6. M. Wang, M. Li, A. Yu, Y. Zhu, M. Yang, C. Mao, *Adv. Funct. Mater.*, 2017, **27**, 1606243-1606259.
7. Q. Dai, C. E. Duty, M. Z. Hu, *Small*, 2010, **6**, 1577-1588.
8. G. Jose, C. Joseph, M .A. Ittyachen, N. V. Unnikrishnan, *Opt. Mater.*, 2007, **29**, 1495-1500.
9. J. McKittrick, L. E. S. Rohwer, *J. Am. Ceram. Soc.*, 2014, **97**, 1327-1352.